Progress In Electromagnetics Research B, Vol. 58, 35–46, 2014

Analysis of Microstrip Line Feed Slot Loaded Patch Antenna Using Artificial Neural Network

Mohammad Aneesh*, Jamshed A. Ansari, Ashish Singh, Kamakshi, and Saiyed S. Sayeed

Abstract—In this article, the parametric analysis of the slot-loaded microstrip line feed patch antenna is investigated using artificial neural network model. The bandwidths of the proposed antenna obtained at TM_{01}, TM_{02}, and TM_{03} frequency modes are 10.2 GHz, 13.6 GHz, and 17.2 GHz, respectively. The performance of the proposed antenna is analyzed using artificial neural network model. The changes obtained in bandwidth due to the position of slot length and slot width are reported. The antenna parameters such as return loss, VSWR, gain and efficiency are also calculated. The simulated results obtained with the help of IE3D simulation software are trained and tested using ANN. Theoretical results are compared with simulated and experimental ones, and they are in close agreement.

1. INTRODUCTION

Microstrip antennas have sparked interest among researchers because of their attractive features like low profile, light weight, and conformal to mounting structures, but they have two most serious limitations, narrow bandwidth and low gain [1]. Available methods for the analysis of MSA have high level of complexity. Generally, there are two methods for analysis of microstrip antenna such as numerical method and analytical method. The numerical methods is complicated compared to analytical methods and require much more time, whereas, analytical methods are easy and specified to only some definite shapes of microstrip antenna. An artificial neural network (ANN) is used here for reducing some of these problems. ANNs are computational tools that learn from experience (training), which provide fast and accurate models for microwave modeling, simulation, and optimization.

Using artificial neural network microstrip patch antenna was reported by Vegni and Toscano [2] in which they proposed the analysis of MSA using artificial neural network. Further, Mishra and Patnaik [3, 4] proposed a CAD model for the design of square patch antenna and artificial model for effective dielectric constant of microstrip line. Later, CAD model using spectral domain formulation [5] was also reported for the designing of rectangular patch antenna. Therefore, Guney and Sarikaya [6] proposed a comparative study of MAMDANI and Sugeno fuzzy interface system models for the resonant frequency calculation of rectangular microstrip patch antenna. Several other papers have also used ANN model to analyze and synthesize the microwave circuits [7–15]. Thakare and Singhal [16] proposed the analysis of broadband slot-loaded inset feed microstrip patch antenna using ANN model. Most of these papers are based on ANN model presented only simulated and experimental results. In this paper, we provide a theoretical investigation and compare its results with simulated and experimental ones.

In this paper, the microstrip line feed slot-loaded patch antenna is proposed. Its theoretical, simulated and ANN results have also been verified experimentally. The proposed antenna is investigated for triple frequency-band operation, so that single antenna can be utilized for more than one frequency bands. The theoretical analysis of the proposed antenna is discussed using circuit theory concept based on modal expansion cavity model whereas ANN used RBFNN model.

Received 11 November 2013, Accepted 25 December 2013, Scheduled 9 January 2014
* Corresponding author: Mohammad Aneesh (aneeshau14@gmail.com).
The authors are with the Department of Electronics & Communication, University of Allahabad, Allahabad, UP 211002, India.

2. ANTENNA DESIGN AND ITS EQUIVALENT CIRCUIT

The geometry of the proposed microstrip line feed slot-loaded antenna is shown in Figure 1. The proposed antenna consists of microstrip line feeding, notches, and it is loaded with two parallel slots. The design specification of antenna is given in the Table 1. The microstrip patch is considered as a parallel combination of resistance (R_1), inductance (L_1) and capacitance (C_1) as shown in Figure 2. The values of R_1, L_1, and C_1 can be calculated as [17],

$$R_1 = \frac{Q_T}{\omega C_1} \tag{1}$$

$$L_1 = \frac{1}{\omega^2 C_1} \tag{2}$$

$$C_1 = \frac{\varepsilon_0 \varepsilon_e LW}{2h} \cos^{-2}\left(\frac{\pi y_0}{L}\right) \tag{3}$$

where L and W are the length and width of the rectangular patch, respectively. y_0 = feed point location and h = thickness of the substrate material.

$$Q_T = \frac{c\sqrt{\varepsilon_e}}{4fh} \tag{4}$$

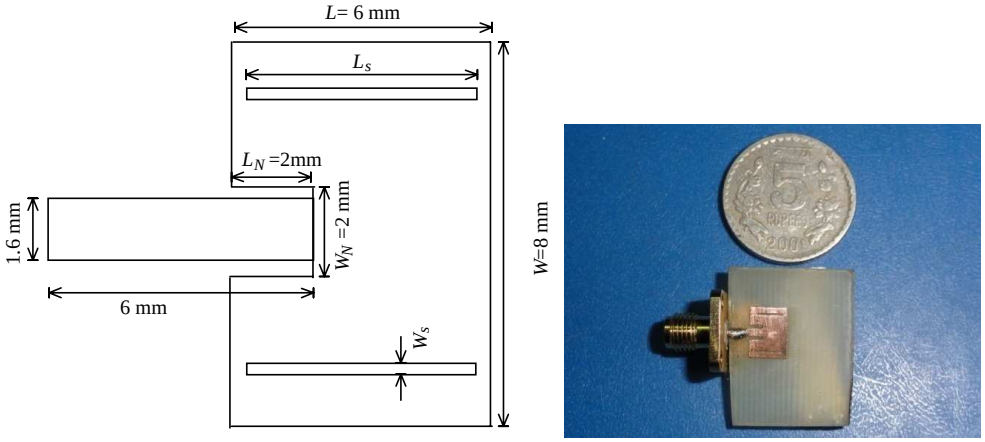

Figure 1. (a) Microstrip line feed slot-loaded MSA. (b) Fabricated proposed design.

Table 1. Design specifications for different configuration of microstrip line feed slot-loaded MSA.

Length of the rectangular patch (L)	6.00 mm
Width of the rectangular patch (W)	8.00 mm
Substrate Thickness (h)	1.57 mm
Length of the notch (L_N)	2.00 mm
Width of the notch (W_N)	2.00 mm
Length of the Slot (L_S)	2.00 mm
Width of the Slot (W_S)	0.20 mm
Length of the Strip Line	6.00 mm
Width of the Strip Line	1.60 mm
Dielectric constant of the material	4.7

where c = velocity of light, f = the design frequency, and ε_e is effective permittivity of the medium, which is given by [17]

$$\varepsilon_e = \frac{\varepsilon_r + 1}{2} + \frac{\varepsilon_r - 1}{2}\left(1 + \frac{10h}{W}\right)^{-\frac{1}{2}} \tag{5}$$

where ε_r is relative permittivity of the substrate material.

Therefore, the impedance of the rectangular patch can be calculated from Figure 2 as

$$Z_P = \frac{1}{\left(\frac{1}{R_1} + \frac{1}{j\omega L_1} + j\omega C_1\right)} \tag{6}$$

In this rectangular patch, a notch ($L_n \times W_n$) is loaded, which causes the flow of two currents in the patch, and one is the normal patch current which causes the antenna to resonate at the design frequency of the initial patch; however, the other current flows around the notch resulting in the second resonance frequency. Discontinuities due to notch incorporated in the patch are considered in terms of an additional series inductance (ΔL) and series capacitance (ΔC) that modify the equivalent circuit of the RMSA as shown in Figure 3, in which ΔL and ΔC can be calculated as [18, 19]

$$L_2 = L_1 + \Delta L \tag{7}$$

$$C_2 = \frac{C_1 \Delta C}{C_1 + \Delta C} \tag{8}$$

The value of R_2 after cutting the notch is calculated similarly as R_1 in [17, 20]. It can be noted that the two resonant circuits, rectangular patch and notch-loaded patch, are coupled through mutual inductance (L_M) and mutual capacitance (C_M). Thus the notch-loaded patch can be considered as shown in Figure 4.

Further, a parallel combination of slot ($L_s \times W_s$) is introduced in the patch geometry. It can be analyzed by the duality relationship between the dipole and slot [21]. The radiation resistance of the slot on the rectangular patch is given as:

$$R_r = \frac{\eta_0 \cos^2 \alpha}{2\pi} \int_0^{\pi} \left[\frac{\left(\cos \frac{k^2 \cos\theta}{2} - \cos \frac{kL_s}{2}\right)^2}{\sin\theta} \right] d\theta \tag{9}$$

where α is inclination angle of the slot ($\alpha = 0^\circ$), and k = wave vector.

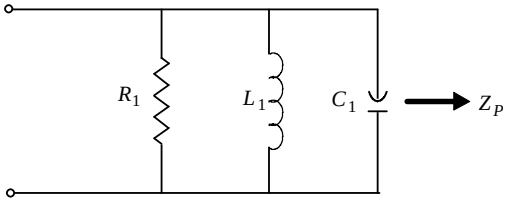

Figure 2. Equivalent circuit of patch.

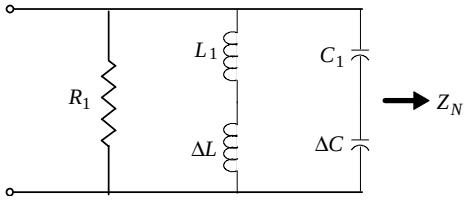

Figure 3. Equivalent circuit of notch.

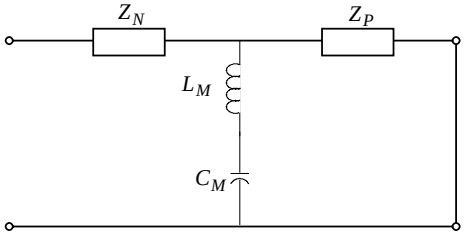

Figure 4. Equivalent circuit of coupled notch loaded patch antenna.

Now the input impedance of the slot for patch [21]

$$Z_s = \frac{\eta_0^2}{4Z_{cy}} \tag{10}$$

where $\eta_0 = 120\pi$ and $Z_{cy} = R_r(kLs) - j[120\{\ln(\frac{L_s}{W_s}) - 1\}\cot(\frac{kL_s}{2}) - X_r(kL_s)]$ in which R_r is the real part and equivalent to radiation resistance of slot, and X_r is the input reactance of the slot [22].

Now the equivalent circuit of the patch is shown in Figure 5.

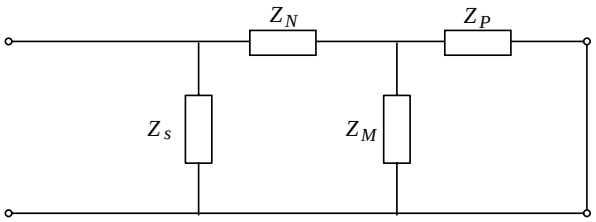

Figure 5. Equivalent circuit of slot-loaded rectangular patch.

The proposed microstrip patch antenna after inserting the microstrip line feed is shown in Figure 6. Hence, the total input impedance of the microstrip line feed slot-loaded rectangular patch can be calculated as

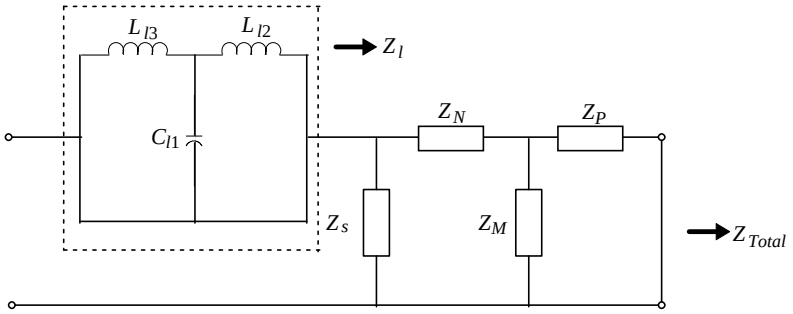

Figure 6. Equivalent circuit of proposed geometry.

$$Z_{Total} = \left(\frac{Z_P Z_M Z_S + Z_N Z_P Z_S + Z_M Z_N Z_S}{Z_P Z_M + Z_N Z_P + Z_M Z_N + Z_P Z_S + Z_M Z_S} + Z_l\right) \tag{11}$$

where Z_P = input impedance of the patch

$$Z_M = \left(j\omega L_M + \frac{1}{j\omega C_M}\right) \tag{12}$$

Z_N = input impedance of the notch loaded patch

$$Z_N = \frac{1}{\left(\frac{1}{R_2} + \frac{1}{j\omega L_2} + j\omega C_2\right)} \tag{13}$$

$$Z_l = \left(\frac{1}{\frac{1}{j\omega L_{l2}} + j\omega C_{l1}} + j\omega L_{l3}\right) \tag{14}$$

Now using Equation (11) one can calculate the total input impedance of the proposed antenna and various antenna parameters such as reflection coefficient, VSWR and return loss as,

$$\text{Reflection coefficient,} \quad \Gamma = \frac{Z_{Total} - Z}{Z_{Total} + Z} \tag{15}$$

where Z is the input impedance of the microstrip fed ($50\,\Omega$).

$$\text{Return loss} \quad RL = 20\log|\Gamma| \tag{16}$$

$$VSWR = \frac{1+\Gamma}{1-\Gamma} \tag{17}$$

$$\text{Bandwidth,} \quad BW = \frac{2\,(f_h - f_l)}{(f_h + f_l)} \times 100\% \tag{18}$$

3. BANDWIDTH SYNTHESIS USING ANN

For the proposed work, radial basis function neural network (RBFNN) is preferred to model the microstrip line feed slot-loaded patch antenna. Feed forward neural networks with a single hidden layer that uses radial basis activation functions for the hidden neurons are called radial basis function networks. RBFNN is applied to various microwave modelling purposes [23, 24]. A typical RBF network structure is shown in Figure 7(a). The parameters C_{ij} and λ_{ij} are centers and standard deviations of radial basis activation functions. Commonly used radial basis activation functions are Gaussian and multiquadratic. The RBF neural network has both types of learning strategies — supervised and unsupervised learning. It consists of input, hidden and output layer of neurons. The hidden layer of neurons represents a series of centers in the input data space. Each of these centers has an activation function. The input x_j and the total input to the ith hidden neurons γ_{ij} are given as [10],

$$\gamma_{ij} = \sqrt{\sum_{j=1}^{n} \frac{(x_j - c_{ij})}{\lambda_{ij}}} \tag{19}$$

where $i = 1, 2, 3, \ldots, N$, and N is the number of hidden neurons. The output value of the ith hidden neuron is $Z_{ij} = \sigma(\gamma_i)$ where $\sigma(\gamma_i)$ is a radial basis function. Finally, the outputs of the RBF network are computed from hidden neurons as shown in Figure 7(a).

$$y_k = \sum_{i=0}^{N} w_{ki} z_{ki} \tag{20}$$

where w_{ki} is the weight of the link between the ith neuron of the hidden layer and the kth neuron of the output layer. Training parameters w of the RBF network include w_{ko}, w_{ki}, c_{ij}, λ_{ij}, $k = 1, 2, \ldots, m$, $i = 1, 2, \ldots, N$, $j = 1, 2, \ldots, n$.

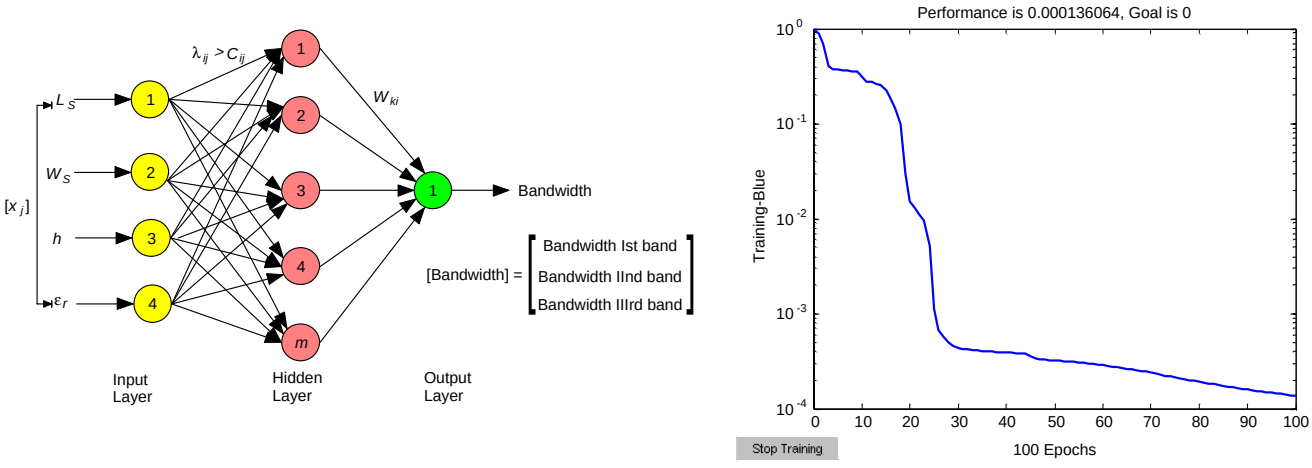

Figure 7. (a) Radial basis function neural network (RBFNN) model. (b) Number of epochs to achieve minimum mean square errors (MSE) for radial basis function neural network (RBFNN).

The RBF network is trained with the data obtained from the mathematical formulation and ZELAND software [25]. Various values of slot length L_S, slot width W_S, height of the substrate h, dielectric constant of the substrate of microstrip line feed slot-loaded patch antenna are used for the training process. In the structure of RBF model, there are 4 input neurons and 1 output neuron used for the analysis of ANN. RBF networks is faster and more accurate for this antenna design. The RBF network automatically adjusts the number of neurons in the hidden layer till the defined accuracy is

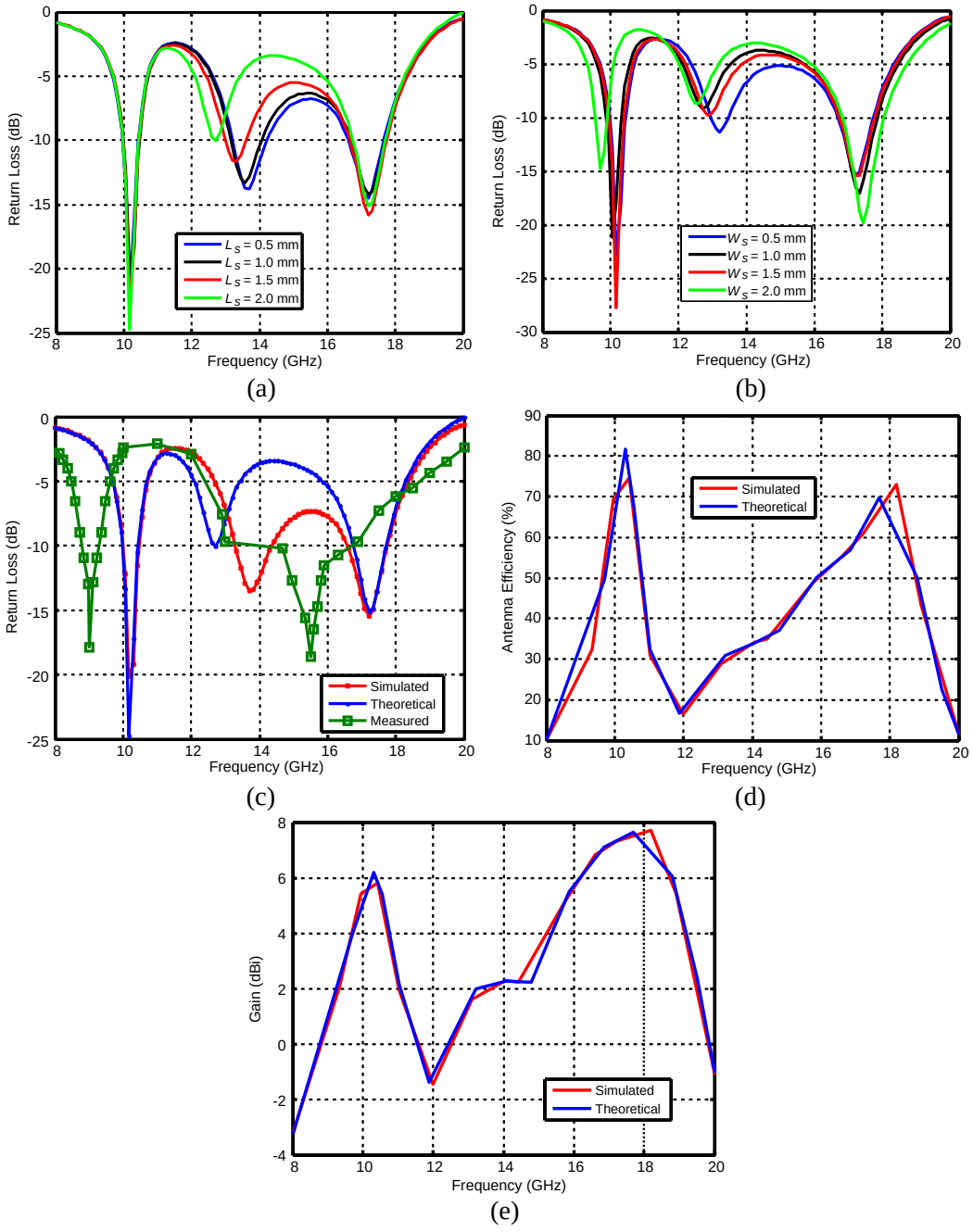

Figure 8. (a) Variation of return loss with slot length (L_s). (b) Variation of return loss with slot width (W_s). (c) Comparison of proposed antenna return loss for simulated, theoretical and measured. (d) Comparison of theoretical and simulated result for antenna efficiency (%) with frequency. (e) Comparison of theoretical and simulated result for gain (dBi) with frequency.

achieved. In the present work, RBFNN model is trained with 40 samples and tested with 21 samples, and the value of spread constant is chosen as 0.01. The network performs training in 20 sec. with 100 epochs.

For the synthesis of bandwidth using RBFNN, 61 training and testing samples are generated with the help of IE3D ZEELAND software, where 40 samples are used for training and remaining 21 samples for testing of RBFNN model. For the training of RBFNN model, four input parameters $[x_j] = [L_s\ W_s\ \varepsilon_r\ h]$ are used, and their respective output parameters are in a 3×1 matrix as shown in Figure 7(a). Training of this model is used for minimizing the error between training output and target output. Figure 7(b) shows that the minimum mean square errors have been achieved with 100 epochs on training of RBFNN model.

4. RESULTS AND DISCUSSION

From Figure 8(a), it is observed that with increasing the length of slot from 0.5 mm to 2.0 mm, the resonance frequency obtained at 10.2 GHz has no significant change whereas band obtained at 13.6 GHz shifts towards lower resonance side. Further, it is also observed that the third band obtained at 17.2 GHz shifts towards higher resonance side. This return loss is due to variation of current length on the patch.

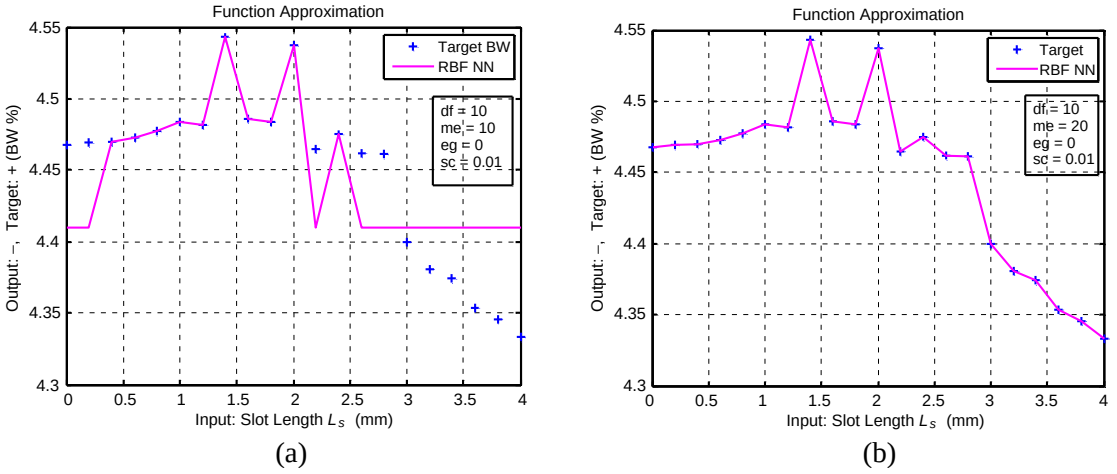

Figure 9. Ist band: variation for (a) 10 Neurons, (b) 20 Neurons.

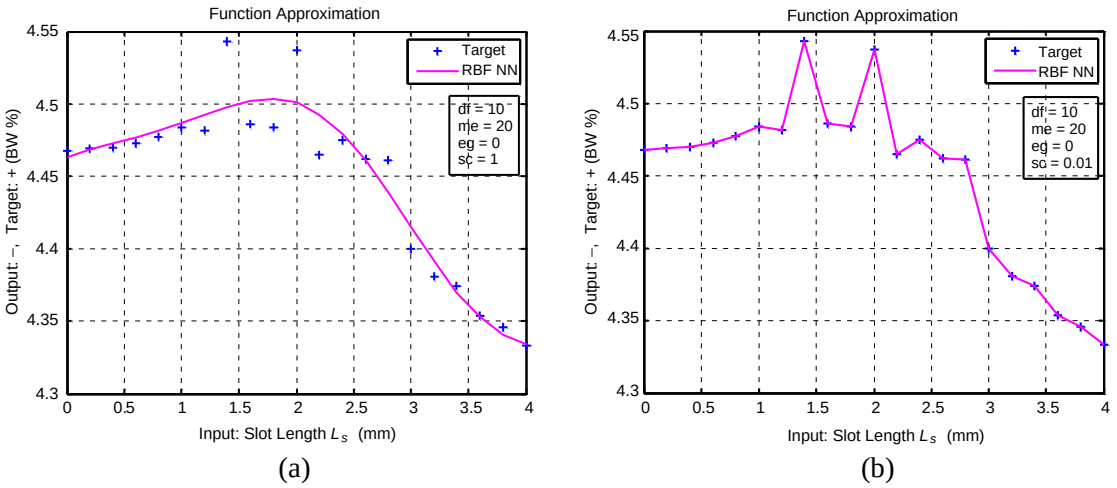

Figure 10. Ist band: variation for (a) spread constant 1, (b) spread constant 0.01.

Figure 8(b) shows the variation of return loss with slot width (W_S). From Figure 8(b), it is observed that with increasing the width of slot from 0.5 mm to 2.0 mm, the resonance frequency obtained at 10.2 GHz (TM_{01}) shifts towards lower resonance side, whereas band obtained at 13.6 GHz (TM_{02}) shifts towards lower resonance side. Further, it is also observed that the third band obtained at 17.2 GHz (TM_{03}) has no significant change. Figure 8(c) shows the comparison among the theoretical, simulated, and experimental results which are in close agreement with each other, and the only variation occurs in experimental results due to irregularity in fabrication of proposed antenna such as size and losses of the solder joints, which are not considered in simulation and theory, which may be the cause of this difference. Figure 8(d) shows that the simulated and theoretical values of antenna efficiency at 10.2 GHz are 78% and 71%, whereas, at 17.2 GHz, they are 73% and 70%, respectively. From Figure 8(e), it is also observed that the gain of the proposed antenna at 10.2 GHz is 6.1 dBi (theoretical) and 6 dBi (simulated), whereas, for the second band at 13.6 GHz it is 2.2 dBi (theoretical and simulated) and third band at 17.2 GHz is 7.8 dBi (simulated) and 7.6 dBi (theoretical). All these values are found in good agreement with theoretical and simulated results.

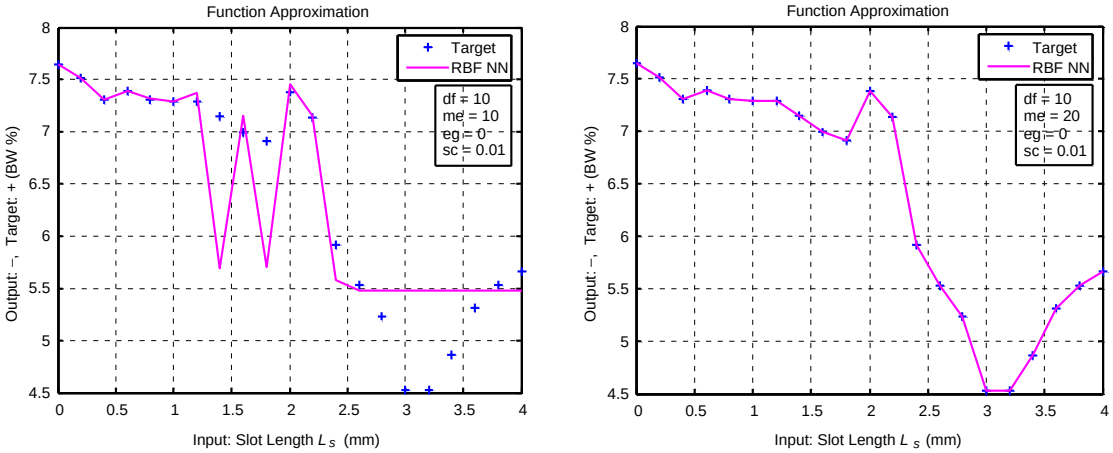

Figure 11. IInd band: variation for (a) 10 Neurons, (b) 20 Neurons.

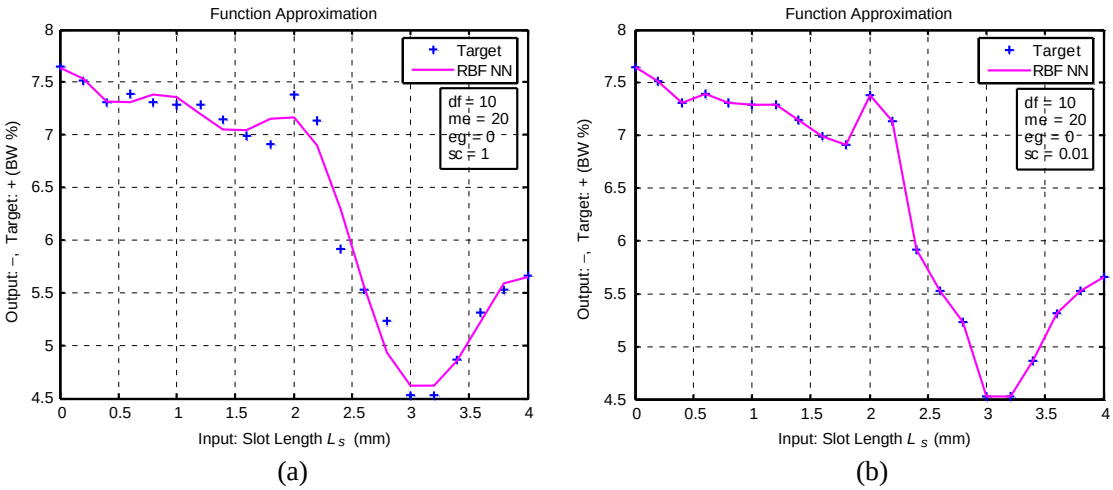

Figure 12. IInd band: variation for (a) spread constant 1, (b) spread constant 0.01.

4.1. Bandwidth Analysis Using RBFNN

Radial basis function neural network is tested with 21 sets of training data. Input layer of RBFNN contains the values of slot length, slot width, dielectric constant, and height of the substrate. Here Figures 9(a)–(b) show the plot of slot lengths versus target bandwidth of the microstrip line feed slot-loaded patch antenna. The values of obtained bandwidth with respect to the slot length have been evaluated with the variation of neurons in hidden layer. Figures 9(a)–(b) show the target bandwidth (%) at 10 and 20 neurons in the hidden layer, where all the other parameters, such as frequency of progress in display (df), error goal (eg), and spread constant (sc), are kept constant. From these figures it is observed that with increasing the number of neurons in the hidden layer, error is minimized, and RBFNN model gives a better accuracy. Hence, the results are in close agreement with the target bandwidth and RBFNN model output. Figures 10(a)–(b) show that the performance of RBFNN model is compared with the variation of spread constant while all other parameters are kept constant.

Figures 11(a)–(b) show the estimation of bandwidth of the second band for the proposed antenna where the input parameters are slot length, slot width, height of the substrate, and dielectric constant. The value of bandwidth with respect to different slot length is evaluated through RBFNN model at 20 neurons. It predicts the accurate value of bandwidth with respect to the target value. The values of bandwidth of the second band with respect to the slot length have been evaluated with the variation of

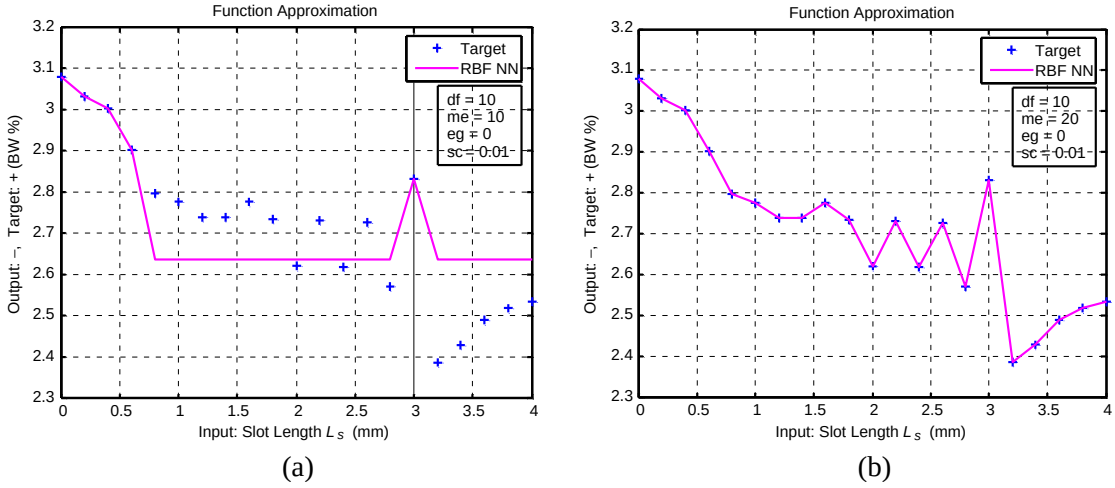

Figure 13. IIIrd band: variation for (a) 10 Neurons, (b) 20 Neurons.

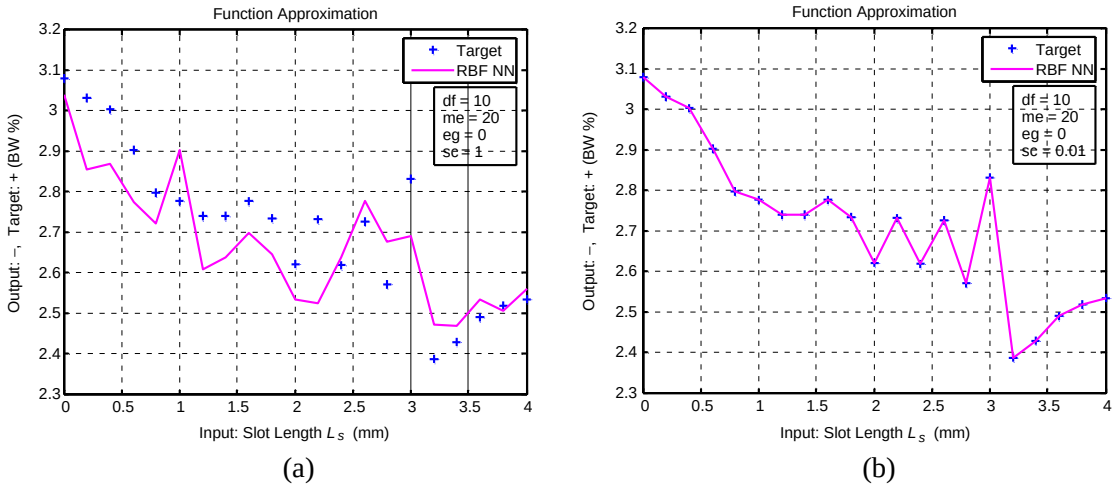

Figure 14. IIIrd band: variation for (a) spread constant 1, (b) spread constant 0.01.

maximum number of neurons. From Figures 12(a)–(b), it is observed that the bandwidth of the second band is accurately determined with the spread constant 0.01.

From Figures 13(a)–(b), it has been further established that the estimated values of the bandwidth of the third band with slot lengths ($L_s = 0$ to 4 mm) are very close to target value with the variation of neurons. Thus, 20 neurons of RBFNN model predict the accurate value of bandwidth with respect to the target value, whereas all other parameters are kept constant (df, eg, sc). Figures 14(a)–(b) show plots between the output target bandwidth and input slot length (L_s). It is observed that with varying the value of spread constant, the output target bandwidth is in close agreement with RBFNN model. The calculated bandwidths for different slot lengths are given in Table 2 and Table 3, which show the compared results of IE3D, theoretical, ANN, and experimental bandwidth for the proposed antenna.

4.2. Comparison of Result of IE3D, ANN and Experiment for the Bandwidth Calculation

Table 2. Value of bandwidth with the variation of slot length.

Slot length L_s (mm)	Slot width W_s (mm)	Bandwidth Ist band	Bandwidth IInd band	Bandwidth IIIrd band	Bandwidth Ist band (RBF NN)	Bandwidth IInd band (RBF NN)	Bandwidth IIIrd band (RBF NN)
0	0	0.04468	0.07644	0.06741	0.04465	0.07641	0.06743
0.2	0.2	0.04469	0.07514	0.06642	0.04465	0.07512	0.06641
0.4	0.2	0.04470	0.07312	0.06578	0.04472	0.07320	0.06575
0.6	0.2	0.04473	0.07389	0.06356	0.04474	0.07390	0.06354
0.8	0.2	0.04477	0.07314	0.06125	0.04476	0.07316	0.06124
1.0	0.2	0.0448	0.07291	0.06080	0.04481	0.07295	0.06081
1.2	0.2	0.04482	0.07284	0.05999	0.04482	0.07287	0.06000
1.4	0.2	0.04543	0.07141	0.060015	0.04546	0.07140	0.06002
1.6	0.2	0.0448	0.0699	0.0608	0.04483	0.07000	0.06083
1.8	0.2	0.0448	0.06911	0.0599	0.04488	0.06921	0.05991
2.0	0.2	0.0453	0.0738	0.0574	0.04531	0.07384	0.05741
2.2	0.2	0.0446	0.0714	0.0598	0.04462	0.07150	0.05982
2.4	0.2	0.04475	0.0592	0.05735	0.04474	0.05930	0.05734
2.6	0.2	0.0446	0.05526	0.0597	0.04464	0.05527	0.05971
2.8	0.2	0.0446	0.0523	0.0563	0.04461	0.05234	0.05631
3.0	0.2	0.0440	0.0453	0.0620	0.04401	0.04534	0.06203
3.2	0.2	0.0438	0.04522	0.0523	0.04381	0.04525	0.05231
3.4	0.2	0.0437	0.04861	0.0532	0.04372	0.04864	0.05322
3.6	0.2	0.0435	0.05310	0.0545	0.04351	0.05319	0.05451
3.8	0.2	0.0434	0.05525	0.0551	0.04341	0.05524	0.05514
4.0	0.2	0.0433	0.056631	0.0555	0.04332	0.05667	0.05555

Table 3. Comparison of results of IE3D, theoretical, ANN, and experiment.

Method	**Ist Band BW**	**IInd Band BW**	**IIIrd Band BW**
Simulated	0.0453	0.0738	0.0574
Theoretical	0.0441	0.0710	0.0561
RBFNN	0.04531	0.07384	0.05741
Experimental (Physically Fabricated)	0.0446	0.0688	0.0628

5. CONCLUSION

An analysis of microstrip line feed slot-loaded patch antenna has been investigated, and the proposed antenna exhibits triple frequency band operation. The results obtained using ANN technique are in close agreement with the experimental ones. The technique utilized for calculating the bandwidth of a microstrip line slot-loaded patch antenna is simple and highly accurate. Thus, the RBFNN technique utilized on the proposed antenna gives substantial accuracy. The proposed antenna exhibits triple band frequency operation at 10.2 GHz, 13.6 GHz, and 17.2 GHz with sufficient bandwidth and moderate gain. This antenna can be used for X-band and Ku-band applications.

ACKNOWLEDGMENT

The author is very grateful to Maulana Azad National Fellowship, University Grant Commission, New Delhi for providing financial assistance through senior research fellowship.

REFERENCES

1. Kumar, G. and K. P. Ray, *Broadband Microstrip Antenna,* Artech House, US, 2003.
2. Vegni, L. and A. Toscano, "Analysis of microstrip antennas using neural networks," *IEEE Trans. Magn.*, Vol. 33, No. 2, 1414–1419, Mar. 1997.
3. Mishra, R. K. and A. Patnaik, "Neural network-based CAD model for the design of square-patch antennas," *IEEE Transactions on Antennas and Propagation*, Vol. 46, No. 12, 1890–1891, Dec. 1998.
4. Patnaik, A. R., K. Mishra, G. K. Patra, and S. K. Dash, "An artificial neural network model for effective dielectric constant of microstrip line," *IEEE Transactions on Antennas and Propagation*, Vol. 45, No. 11, 1697, Nov. 1997.
5. Mishra, R. K. and A. Patnaik, "Designing rectangular patch antenna using the neuro spectral method," *IEEE Transactions on Antennas and Propagation*, Vol. 51, No. 8, 1914–1921, Aug. 2003.
6. Guney, K. and N. Sarikaya, "Comparison of MAMDANI and Sugeno fuzzy inference system models for resonant frequency calculation of rectangular microstrip antennas," *Progress In Electromagnetics Research B*, Vol. 12, 81–104, 2009.
7. Watson, P. M. and K. C. Gupta, "Design and optimization of CPW circuits using EM ANN models for CPW components," *IEEE Trans. Microwave Theory Techniques*, Vol. 45, No. 12, 2515–2523, Dec. 1997.
8. Zaabab, A. H., Q. J. Zhang, and M. Nakhla, "Analysis and optimization of microwave circuits & devices using neural network models," *IEEE MTT-S Digest*, Vol. 1, 393–396, 1994.
9. Naser-Moghaddasi, M., P. D. Barjoei, and A. Naghsh, "Heuristic artificial neural network for analysing and synthesizing rectangular microstrip antenna," *IJCSNS International Journal of Computer Science and Network Security*, Vol. 7, No. 12, 278–281, Dec. 2007.
10. Täurker, N., F. Gäunes, and T. Yildirim, "Artificial neural design of microstrip antennas," *Turk. J. Elec. Engin.*, Vol. 14, No. 3, 445–453, 2006.
11. Peik, S. E., G. Coutts, and R. R. Mansour, "Application of neural networks in microwave circuit modelling," *IEEE Canadian Conference on Electrical and Computer Engineering*, Vol. 2, 928–931, May 24–28, 1998.
12. Devi, S., D. C. Panda, and S. S. Pattnaik, "A novel method of using artificial neural networks to calculate input impedance of circular microstrip antenna," *Antennas and Propagation Society International Symposium*, Vol. 3, 462–465, Jun. 16–21, 2002.
13. Karaboga, D., K. Guney, S. Sagiroglu, and M. Erler, "Neural computation of resonant frequency of electrically thin and thick rectangular microstrip antennas," *IEEE Proceedings, Microwaves, Antennas and Propagation*, Vol. 146, No. 2, 155–159, Apr. 1999.

14. Guney, K. and N. Sarikaya, "Resonant frequency calculation for circular microstrip antennas with a dielectric cover using adaptive network-based fuzzy inference system optimized by various algorithms," *Progress In Electromagnetic Research*, Vol. 72, 279–306, 2007.
15. Pattnaik, S. S., D. C. Panda, and S. Devi, "Radiation resistance of coax-fed rectangular microstrip antenna using artificial neural networks," *Microwave and Optical Technology Lett.*, Vol. 34, No. 1, 51–53, Jul. 5, 2002.
16. Thakare, V. V. and P. K. Singhal, "Bandwidth analysis by introducing slots in microstrip antenna design using ANN," *Progress In Electromagnetics Research M*, Vol. 9, 107–122, 2009.
17. Bahal, I. J. and P. Bhartia, *Microstrip Antennas*, Artech House, Boston, MA, 1985.
18. Pandey, V. K. and B. R. Vishvakarma, "Theoretical analysis of linear array antenna of stacked patches," *Indian J. Radio & Space Phys.*, Vol. 3, 125–127, 2005.
19. Meshram, M. K. and B. R. Vishvakarma, "Gap-coupled microstrip array antenna for wide band operation," *Int. J. Electronics*, Vol. 88, 1161–1175, 2001.
20. Wang, E., J. Zheng, and Y. Liu, "A novel dualband patch antenna for WLAN communication," *Progress In Electromagnetics Research C*, Vol. 6, 289–291, 2009.
21. Wolf, E. A., *Antenna Analysis,* Artech house, Narwood, US, 1998.
22. Ansari, J. A., A. Mishra, and B. R. Vishvakarma, "Half U-slot loaded semicircular disk patch antenna for GSM mobile phone and optical communications," *Progress In Electromagnetics Research C*, Vol. 18, 31–45, 2011.
23. Aneesh, M., J. A. Ansari, A. Singh, K. Kamakshi, and S. Verma, "RBF Neural Network Modeling of Rectangular Microstrip Patch Antenna," *2012 Third International Conference on Computer Comm. Technology*, 241–244, 2012, Doi: 10.1109/ICCCT.2012.56.
24. Guney, K. and N. Sarikaya, "Adaptive neuro-fuzzy inference system for the input resistance computation of rectangular microstrip antennas with thin and thick substrates," *Journal of Electromagnetic Waves and Applications*, Vol. 18, No. 1, 23–39, 2004.
25. IE3D simulation software, Version 14.05, Zeeland, 2008.